World Conference on Timber Engineering Oslo 2023

NAIL-LAMINATED TIMBER-CONCRETE COMPOSITE BEAMS WITH NOTCHED CONNECTIONS AND STEEL FIBRE REINFORCEMENT

Hamidreza Chaboki [1], Lei Zhang [2], Thomas Tannert [3], Jianhui Zhou [4]

ABSTRACT: The utilization of timber-concrete composite (TCC) floors, which involves connecting a wood beam or panel to a concrete layer via shear connectors, has experienced a surge in popularity in recent years. Although notched connections have proven to be cost-effective shear connections, without proper concrete reinforcement, cracks can develop in the notched area and ultimately lead to brittle shear failure. In this paper, we present research aimed at mitigating crack growth in concrete and preventing notch shear failure in concrete by employing steel fibre reinforcement. Eight groups of nail-laminated TCC beams with varying notch depth, location and number of notches, and thickness ratio of concrete to timber were tested under third-point bending. The results demonstrated that the number of notches and thickness ratio had the greatest impact on beam bending properties, while the influence of notch location and depth was marginal. Furthermore, the steel fibres effectively delayed crack propagation in the concrete notches, resulting in timber failure in all tested specimens. The notches cut on NLT and filled with concrete affect the modulus of elasticity of NLT and need to be considered for the calculation of composite efficiency and effective TCC beam bending stiffness.

KEYWORDS: Timber-concrete composite floor, Bending performance, Notched connection, Steel fibres

1 INTRODUCTION

1.1 Background

Timber-concrete composite (TCC) floors exhibit enhanced bending stiffness and load-carrying capacity compared to pure timber floors of the same depth, enabling longer spans. The combination of a concrete layer to resist compression and timber to resist tension results in efficient utilization of the mechanical properties of both materials. In addition, TCC floors offer superior fire resistance, vibration damping, and acoustic performance compared to bare timber floors [1-5].

Shear connections are integral to generating composite action between the materials in TCC. Various types of connections have been tested, including self-tapping screws and glued-in steel mesh plates [5]. However, these metal fasteners can be disadvantageous in terms of constructability, cost, and labour intensity. Notched connections, prefabricated using computer numerical control machines, offer a potential solution, as they allow for precise, rapid, and cost-effective production with minimal use of metal fasteners [4]. However, the reduction of the cross-sectional area due to the notches impacts the bending capacity and stiffness of the TCC floors [6]. The TCC floor bending stiffness and strength are also influenced by the number and locations of notches, as well as the presence of additional steel fasteners [7]. Up to date, the notched connections are not standardized in the TCC floor design.

Zhang et al. [7] conducted a parametric study to investigate the impact of various geometry-related factors such as depth and number of notches, timber shear length, and concrete thickness on the bending stiffness of TCC floors. Their findings suggest that optimizing the number, location, and size of notches can lead to high composite efficiency in the TCC system. Shi et al. [6] examined the shear behavior of notched connections and observed that when the length of the notch increased from 150 mm to 250 mm, the failure mode changed from shear failure of concrete in the notch to compression failure of timber in front of the notch. Zhang et al. [8] developed an analytical method involving a simple release-and-restore procedure to predict stress distribution and slip between timber and concrete while considering the discrete and semi-rigid features of the notched connections.

The high stiffness of notched connections allows the notches to be spaced along the beam at a large distance, making the concrete layer susceptible to cracking due to stress concentration at the notches. The cracking of concrete can lead to brittle failure and a reduction in beam load-carrying capacity, especially in the absence of reinforcement [9,10]. To address these issues, additional screws are often used to take the tensile forces and restrict crack opening and uplifting [11,12]. Alternatively, micro-notches with millimetre dimensions can be milled into the timber surface to improve continuous shear transfer and reduce uplifting forces [13]. Müller and Frangi [13] showed that micro-notches can achieve close-to-full

[1] Hamidreza Chaboki, University of Northern British Columbia, Canada, chaboki@unbc.ca
[2] Lei Zhang, University of Northern British Columbia, Canada, lzhang2@unbc.ca
[3] Thomas Tannert, University of Northern British Columbia, Canada, thomas.tannert@unbc.ca
[4] Jianhui Zhou, University of Northern British Columbia, Canada, jianhui.zhou@unbc.ca

https://doi.org/10.52202/069179-0421

composite action and sufficient shear strength for common residential and office buildings.

In concrete structures, steel fibres are often used as reinforcement to reduce crack formation and control propagation. These fibres connect and bridge gaps in the concrete during hardening, delaying crack growth and reducing crack width [14]. It is advantageous to strength the concrete layer in TCC with steel fibres to restrict the crack opening and prevent shear failure of notched connections.

1.2 OBJECTIVES

In this study, the bending performance of nail-laminated timber-concrete composite beams with notched connections and steel fibre reinforcement was investigated. Third-point bending tests were conducted on eight groups of nails-laminated TCC beams, each featuring varying notch depth, location, and number of notches, as well as thickness ratios of concrete to timber layers, to investigate the variation of notches on the bending performance of the beams, as well as the efficacy of steel fibres in mitigating brittle failure of notched connections. The effect of notches on the modulus of elasticity of NLT for calculating the composite efficiency of TCC was also evaluated.

2 EXPERIMENTAL INVESTIGATIONS

2.1 SPECIMEN CONFIGURATIONS

A total of 24 TCC beams, divided into eight groups, with three replicates in each group, were constructed and tested. The beams had a width of 190 mm, a length of 3.06 m (span of 2.9 m), and a total thickness of 150 mm. The number, depth, and location of notches varied among the groups are shown in Table 1 and illustrated in Figure 1. The notches were symmetrically positioned about the mid-span of beams.

To prevent layer separation, three self-tapping screws with a diameter of 8 mm were inserted into each specimen at the mid-span and two ends, as illustrated in Figure 2. The screws, which had an embedment length of 50 mm in both wood and concrete, were made of carbon steel with a zinc coating. In the case of SP7, the thicker timber layer required a longer embedment length of 60 mm into the wood.

Table 1: *Specification of specimens*

Group	Concrete to timber thickness ratio	Number of notches	Notch depth (mm)
SP1	2:3	2	20
SP2	2:3	2	20
SP3	2:3	4	20
SP4	2:3	4	30
SP5	2:3	4	40
SP6	2:3	4	15-25
SP7	1:2	4	20
SP8	1:1	4	20

The reference group SP3 had a concrete thickness of 60 mm and a timber thickness of 90 mm, with four notches that were 20 mm deep and 150 mm long. To explore the impact of the number of notches on the stiffness and strength of the TCC beams, SP1 and SP2 featured only two notches that were 20 mm deep and spaced 1800 mm and 1200 mm apart, respectively. The location and length of notches in SP4 and SP5 were identical to those of the reference group, but the depths of the notches were 30 mm and 40 mm deep, respectively. In SP6, the notch depth varied along the beam length, with a depth of 25 mm near the supports and 15 mm near the mid-span. Finally, SP7 and SP8 were similar to the control group but differed in their timber-to-concrete thickness ratios. The thickness of timber and concrete in the specimens ranged from 75-100 mm and 50-75 mm, respectively.

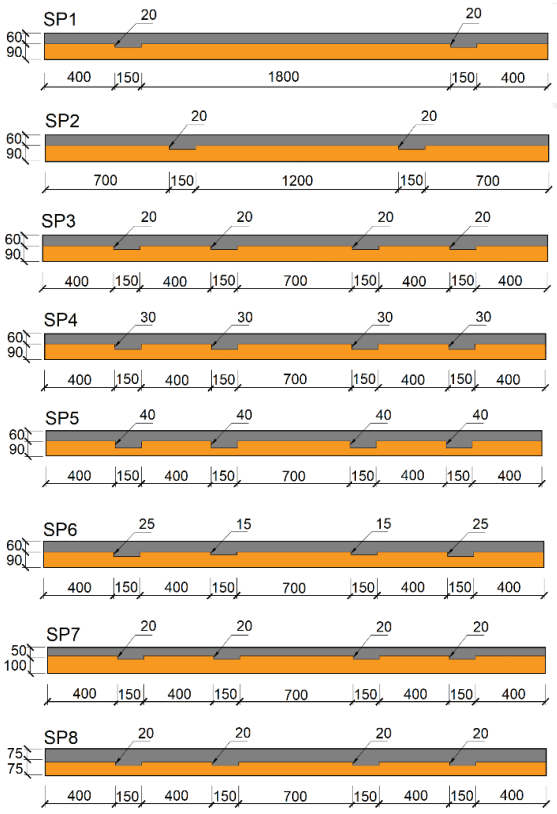

Figure 1: *Nail-laminated timber-concrete composite beam configurations (dimensions in mm)*

2.2 MATERIALS

Five 38 mm thick spruce-pine-fir (SPF) lumber planks of grade No. 2 were nailed together (6d, 3 inches long, one row @ 120 mm spacing) to fabricate the nail-laminated timber (NLT) beams. The lumber had an average density of 444 kg/m^3 and a moisture content of 13% before testing. The notches on NLT were cut using a router. The moduli of elasticity (MOE) of the NLT beams were measured before (E_t) and after ($E_{t,notched}$) cutting the notches by non-destructive centre-point bending tests.

https://doi.org/10.52202/069179-0421

The average measured MOE values of each NLT group are listed in Table 2, which indicates different levels of MOE reduction after notching (11% to 62%). SP5 with the deepest notches showed the highest drop in MOE while SP1 with the minimal number of notches showed the lowest reduction. The choice of MOE on the composite efficiency and the bending stiffness of TCC are discussed in the results section.

Table 2: *Average MOE values of NLT beams*

Group	E_t (MPa)	$E_{t,notched}$ (MPa)	$E_{t,n\&c,FEM}$ (MPa)
SP1	7802	6907	7027
SP2	9618	7291	7921
SP3	7931	5941	6855
SP4	7900	4451	5488
SP5	8615	3311	4685
SP6	7677	6208	6622
SP7	8316	6493	6605
SP8	9790	6460	7925

Note: E_t is the MOE of NLT tested without notches; $E_{t,notched}$ is the MOE of NLT tested with notches; $E_{t,n\&c,FEM}$ is the MOE of NLT determined from the finite element model.

Figure 2: *Specimen preparation A) NLT with notches and screws B) Formwork for concrete casting C) After concrete curing*

The specimen preparation process is shown in Figure 2. To avoid the formation of voids around the corners of notches, the nominal maximum coarse-aggregate size in concrete was chosen as 10 mm. All the specimens were made from the same batch of concrete. To reinforce the concrete layer, HE-4550 steel fibres with 50 mm length and two bend ends were used in a volume reinforcement ratio of 0.5%. Three cylinders with a nominal diameter of 100 mm and a height of 200 mm were cast at the same time and tested according to ASTM C39/C39M-20 [15] after 28 days. The average compressive strength of concrete cylinders was 39.3 MPa, with a coefficient of variation of 1%. Concrete cylinders had a density of 2,325 kg/m^3. The Young's modulus of concrete was estimated as 28027 MPa based on the 28-day compressive strength (f_c') and density (γ_c) applying Eq. (1) [16]:

$$E_c = (3300\sqrt{f_c'} + 6900)(\frac{\gamma_c}{2300})^{1.5} \quad (1)$$

2.3 FINITE ELEMENT MODELS

2D finite element models of the NLT beams were developed in the general-purpose finite element software ABAQUS [17] to numerically evaluate MOE of the notched NLT with concrete filled in notches ($E_{t,n\&c,FEM}$). The contact between timber and concrete in the tangential direction was defined as penalty with a coefficient friction of 0.6 [18] and a hard contact in the normal direction. The model was verified for both solid and notched NLT beams. The results of MOE for the notched NLT filled with concrete are shown in Table 2. Compared to NLT without notches, the reduction of MOE with notches filled with concrete ranges from 10% to 46% depending on the notch configurations.

2.4 METHODS

The TCC beams were tested under three-point bending based on ASTM 198-15 [19], as illustrated in Figure 3. The supports were 100 mm wide to avoid indentation of wood. Two string potentiometers were used to measure the mid-span deflection, and four LVDTs were installed at two ends of each beam on both sides to measure the relative slip between timber and concrete. The deflection and load were recorded for calculating the bending stiffness and moment capacities. The displacement-controlled load was applied at a rate of 3 mm/min to ensure the specimens failed in roughly 20 minutes.

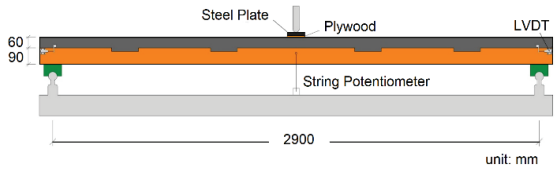

Figure 3: *Schematic of the bending test setup*

The serviceability bending stiffness (referred to as bending stiffness herein) of the floors was determined from Eq. (2) [19]:

$$EI = \frac{PL^3}{48\Delta} \quad (2)$$

where L is span and P/Δ is the slope of the load-deflection curve between 10% and 40% of peak load, regarded as the load level at serviceability limit states [20].

Eq. (3) was used to determine the ultimate bending stiffness of the beams [19]:

$$EI_{ult} = \frac{L^3}{48}\frac{0.8P_{max}}{\Delta_{0.8}} \quad (3)$$

https://doi.org/10.52202/069179-0421

where $\Delta_{0.8}$ indicates the mid-span deflection at 80% of the peak load [20].

The composite efficiencies of the tested TCC beams were evaluated by comparing them with non-composite and full composite TCC beams. The theoretical bending stiffness of a non-composite floor can be calculated using Eq. (4), where E_c and E_t are the concrete and timber moduli of elasticity, respectively; and I_c and I_t are the concrete and timber second moments of area, respectively [21].

$$EI_{no} = E_c I_c + E_t I_t \tag{4}$$

The bending stiffness for the theoretical full composite floor is determined according to Eq. (5) [21]

$$EI_{full} = E_c I_c + E_t I_t + \frac{\left(\frac{h_c + h_t}{2}\right)^2}{\frac{1}{E_c A_c} + \frac{1}{E_t A_t}} \tag{5}$$

where A_c and A_t are the cross-section areas of concrete and timber, respectively; and h_c and h_t are the concrete and timber depths, respectively.

The deflection-based composite efficiency [21] is calculated according to Eq. (6):

$$\lambda = \frac{\Delta_{no} - \Delta}{\Delta_{no} - \Delta_{ful}} = \frac{\frac{1}{EI_{no}} - \frac{1}{EI}}{\frac{1}{EI_{no}} - \frac{1}{EI_{full}}} \tag{6}$$

where Δ_{no}, Δ_{ful}, and Δ are the deflections of the non-composite, full composite, and tested beams under the same load (10% - 40% of peak load).

3 RESULTS AND DISCUSSION

3.1 LOAD-DEFLECTION RELATIONSHIPS & FAILURE MODES

The load-deflection curves and failure modes for each group are presented in Figures 4 and 5, respectively. As the load increased, the TCC beams deformed elastically at the beginning and then exhibited nonlinear deformation after surpassing certain load levels. Concrete shear cracks formed around notches and propagated diagonally or nearly vertically after reaching certain load levels, but the steel fibers limited the extent of crack opening. Since the NLT beams were attached using nails, the lumber planks failed individually, causing multiple peaks and drops in the load-deflection curves.

The failure modes of the specimens are summarized in Table 3. The majority of TCC beams failed in the timber layer due to tension or combined bending and tension, as shown in red circles in Figure 5. Notched connection configurations and the relative thicknesses of timber and concrete in TCC beams did not significantly impact the failure patterns.

In terms of concrete failure, almost all specimens had diagonal concrete cracking at the notched corners (shear cracks) that started in a diagonal or almost vertical orientation, then spread horizontally. Once the first timber bending failure happened, a gap between timber and concrete was formed. With more lumber failure and an increase in deflection, the notched connections in the concrete portion were sheared off, starting with one external notch near the support and then the internal notch on the same side. The failure of the notches caused the failure of the concrete layer.

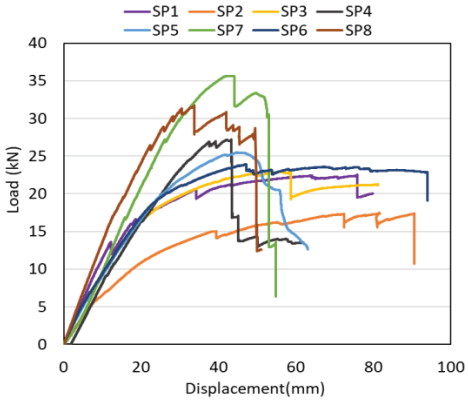

Figure 4: *Typical load-deflection curves of each group*

Figure 5*: Failure patterns of NLTCC beams under bending*

The specimens SP1, SP7, and SP8 with the same notched connections but different concrete-to-timber thickness

ratios exhibited slightly different failure patterns. SP1 experienced timber bending failure at mid-span without visible damage to the concrete layer. SP7 was able to withstand a higher load even after two lumber planks failed by bending. The steel fibres controlled the crack width in the concrete, resulting in higher loads and buckling failure of the concrete. In SP8, after the timber failure, concrete was buckled under compression. It is worth noting that the steel fibres limited the crack width and provided ductility. The progressive failure in NLT and the reinforcement of concrete using steel fibres are believed to be the reasons for the ductile behaviour observed in these groups.

Table 3: *Nail-laminated TCC beam failure modes*

Group	Failure mode
SP1	Timber combined bending and tensile failure
SP2, SP3 SP4, SP5 SP6	Timber combined bending and tensile failure & notch shear failure in concrete
SP7 SP8	Timber combined tensile and bending failure, notch shear failure in concrete & concrete buckling

3.2 BENDING PROPERTIES

The bending properties including the average peak load (P_{max}), bending stiffness (EI), ultimate bending stiffness (EI_{ult}), and bending stiffness reduction are listed in Table 4. Comparing load-carrying capacities among different groups, groups SP1 and SP2 exhibited similar load-carrying capacities, approximately 18.5 kN; Groups SP3-6 exhibited similar load-carrying capacities at around 24.0 kN; Groups SP7 and SP8 exhibited the highest load-carrying capacities of 32.5 kN. Comparing groups SP1-6, all of which had the same total beam thickness and concrete-to-timber thickness ratio, it is apparent that the number of notches had a positive impact on the floor load-carrying capacity. Interestingly, the depth of notches between 15 mm and 40 mm did not affect the load-carrying capacity when comparing groups SP3-6. No clear trend can be observed concerning the impact of the thickness ratio of concrete to timber on the strength properties of beams.

The notch configuration had slightly different effects on the serviceability and ultimate bending stiffness of beams. SP1,3-5 have similar serviceability bending stiffness values from 438 to 458 kNmm^2, while those of SP2 and SP6 had lower values from 382 to 398 kNmm^2. Although the NLT beams had higher bending stiffness in SP2 and SP6 (shown in Table 2), the lower connection stiffness in the two specimen series resulted in lower bending stiffness of composite beams. SP8 has the highest bending stiffness owing to the highest concrete-to-timber thickness ratio. However, the second-highest bending stiffness was observed in SP7 which had the lowest concrete-to-timber thickness ratio. It should be noted that small cracks can happen in concrete while moving the TCC beams before testing, and workmanship was not the same in all the specimens. SP7 seems to be the group with the highest quality, making it difficult to investigate the effect of notch configurations on beam bending stiffness.

The reduction of stiffness from serviceability state (EI) to ultimate state (EI_{ult}) varies among the groups from 1.4% to 28.0% without a clear pattern. Further analysis of the slip between the two layers in each group is required, as the notch configurations may have an impact on the actual connection stiffness in each group.

Table 4: *Summary of peak load and bending stiffness*

Group	P_{max} (kN)	EI (kNm^2)	EI_{ult} (kNm^2)	Reduction of stiffness
SP1	19.0	439	432	1.4%
SP2	18.0	382	274	28.0%
SP3	23.7	458	343	26.1%
SP4	25.5	458	394	13.8%
SP5	23.4	438	383	12.6%
SP6	25.3	398	382	3.6%
SP7	33.4	578	533	8.0%
SP8	31.9	684	581	15.2%

3.3 COMPOSITE EFFICIENCY

The calculated deflection-based composite efficiencies of the composite beams according to Eq. (6) are presented in Figure 6. The values are computed with different MOE values of NLT beams listed in Table 2. The values in blue are calculated based on the measured E_t of NLT beams without notches; values in red were based on the measured $E_{t,notch}$ of NLT beams with notches; and values in grey were based on $E_{t,n\&c,FEM}$ of NLT beams with notches filled with concrete determined from finite element models. The trend of composite efficiency among groups is similar to that of the serviceability bending stiffness. Groups SP7 and SP8 had higher composite efficiencies than the rest of the groups, while group SP2 has the lowest composite efficiency.

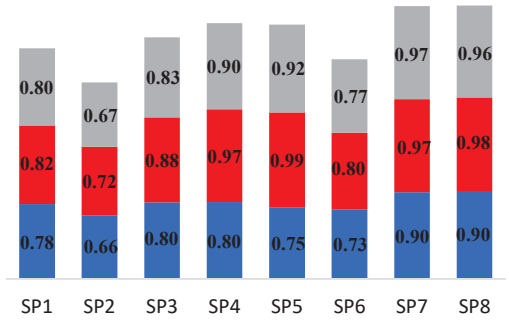

Figure 6: *Composite efficiency of deflection using different timber modulus of elasticity*

Not surprisingly, the higher the MOE used, the lower the composite efficiency was determined. The choice of MOE values of NLT beams can lead to different judgments of composite efficiency and composite action. For instance, for group SP5, the composite efficiency using the measured $E_{t,notch}$ is 24% higher than that using the

https://doi.org/10.52202/069179-0421

measured E_t, and is 7% higher than that using the $E_{t,n\&c,FEM}$. The same issue of choosing MOE of timber will arise when it comes to the prediction of bending stiffness of TCC beams with notches, which should be considered in the design practice.

4 CONCLUSIONS

The bending properties of 24 NLT-concrete composite beams with varied notched configurations and steel fibre reinforcement were investigated experimentally in this work. The following conclusions can be derived: 1) The notch number and concrete-to-timber ratio had major impacts on the beam bending performance, while notch location and depth had marginal impact. 2) The use of steel fibres can postpone shear failure in concrete and ensure a more controllable timber bending failure. 3) The effect of notches on the MOE of timber can lead to different interpretations of composite efficiency and prediction of bending stiffness of composite beams.

ACKNOWLEDGEMENT

This project was supported through an NSERC Discovery Grant and the BC Forestry Innovation Investment –Wood First program. The authors appreciate the technical support from the technicians at the Wood Innovation Research Laboratory at UNBC.

REFERENCES

[1] Higgins, C., Barbosa, A. R., Blank, C. 2017. Structural tests of concrete composite-cross-laminated timber floors. Rep. No. 17-01. Corvallis, OR: Oregon State University.

[2] Martins, C., Santos, P., Almeida, P., Godinho, L., Dias, A. 2015. Acoustic performance of timber and timber-concrete floors. Construction and Building Materials, 101: 684–691.

[3] Mai, K. Q., Park, A., Nguyen, K. T., Lee, K. 2018. Full-Scale Static and Dynamic Experiments of Hybrid CLT–Concrete Composite Floor. Construction and Building Materials, 170: 55–65.

[4] Zhang L., Chui Y. H., Tomlinson D. 2020. Experimental investigation on the shear properties of notched connections in mass timber panel-concrete composite floors. Construction and Building Materials, 234: 117375.

[5] Yeoh, D., Fragiacomo, M., De Franceschi, M., Heng Boon K. 2011. State of the Art on Timber-Concrete Composite Structures: Literature Review. Journal of Structural Engineering, 137(10): 1085-1095.

[6] Shi, D., Hu, X., Du, H., Xie, Z., Meng, Y. 2021. Study on shear performance of notched connections for glulam-concrete composite beams under fire. Fire Safety Journal, 126: 103482.

[7] Zhang, L., Zhou, J., Zhang, S., Chui, Y. H. 2022. Bending stiffness prediction to mass timber panel-concrete composite floors with notched connections. Engineering Structures, 262: 114354.

[8] Zhang, L., Zhang, S., Chui, Y. H. 2021. Analytical evaluation to the timber-concrete composite beam connected with notched connections. Engineering Structures, 227: 111466.

[9] Jiang, Y., Crocetti, R. 2019. CLT-concrete composite floors with notched shear connectors. Construction and Building Materials, 195: 127-139.

[10] Dias, A., Schänzlin, J., Dietsch, P. 2018. Design of timber-concrete composite structures. COST Action FP1402/WG 4, Shaker Verlag Aachen.

[11] Boccadoro, L., Steiger, R., Zweidler, S., Frangi, A. 2017. Analysis of shear transfer and gap opening in timber-concrete composite members with notched connections. Materials and Structures, 50(5): 1–15.

[12] Boccadoro, L., Zweidler, S., Steiger, R., Frangi, A. 2017. Bending tests on timber-concrete composite members made of beech laminated veneer lumber with notched connection. Engineering Structures, 132: 14–28.

[13] Müller, K., Frangi, A. 2021. Micro-notches as a novel connection system for timber-concrete composite slabs. Journal of Engineering Structures, 245: 112688.

[14] Ghalehnovi, M., Karimipour, A., de Brito, J., Chaboki, H. 2020. Crack width and propagation in recycled coarse aggregate concrete beams reinforced with steel fibres. Applied Sciences, 10(21): 75-87.

[15] ASTM. 2020. Standard test method for compressive strength of cylindrical concrete specimens. ASTM C39/C39M-20. West Conshohocken, PA: ASTM.

[16] CSA. 2019. Design of concrete structures. CSA A23.3-19. Mississauga, ON, Canada.

[17] ABAQUS/CAE. 2017. User's Manual. Dassault Systeme Simulia.

[18] Jaaranen, J., Fink, G. 2020. Friction behaviour of timber-concrete contact pairs. Construction and Building Materials, 243: 118273-118282.

[19] ASTM. 2015. Standard test methods of static tests of lumber in structural sizes. ASTM D198-15. West Conshohocken, PA: ASTM.

[20] CEN. 1991. Timber structures — Joints made with mechanical fasteners — General principles for the determination of strength and deformation characteristics. EN 26891. Brussels, Belgium: CEN.

[21] Zhang, L., Zhou, J., Chui, Y. H., Tomlinson, D. 2022. Experimental Investigation on the Structural Performance of Mass Timber Panel-Concrete Composite Floors with Notched Connections. Journal of Structural Engineering, 148: 04021249.